

Novel electroceramics related to CaTiO_3 sintered with the aid of MgF_2 and LiF

S. Nemouchi, L. Taïbi-Benziada

Faculty of Chemistry, USTHB, P.O. Box 32 El-Alia, Bab-Ezzouar, 16311 Algiers, Algeria

Abstract

CaTiO_3 was synthesized by solid-state reaction between CaCO_3 and TiO_2 (rutile) at 850°C . Pellets of $(1-x) \text{CaTiO}_3 + x \text{MgF}_2 + x \text{LiF}$ were sintered at 900°C for 2h. XRD patterns and SEM observations were collected at room temperature. DSC analyses and dielectric measurements were carried out to investigate the phase transitions in these new oxyfluorides. Novel perovskite phases with general formula $\text{Ca}_{1-x}\text{Mg}_x(\text{Ti}_{1-x}\text{Li}_x)\text{O}_{3-3x}\text{F}_{3x}$ ($0 \leq x \leq 0.25$) are obtained and 1 or 2 structural transformations are detected in these fluorinated materials.

1. Introduction

The perovskite-type compounds ABO_3 arouse a great interest for several applications thanks to their easy synthesis by solid state reaction, sol-gel or hydrothermal method and their properties. Due to their high relative permittivities, these materials are mostly used in the electronics industry. For a long time, most of the research was focussed on ferroelectric BaTiO_3 -based and paraelectric SrTiO_3 -based ceramics, which have been extensively utilized to manufacture low-frequency electronic devices. For the last decade, the expansion of microwave technologies induced the need of a new generation of dielectric materials and CaTiO_3 -based materials attracted many researchers to investigate the synthesis and the physical properties of this perovskite [1,2]. Whatever, it was well known from many years ago that calcium titanate can be used for the treating and the storage of nuclear wastes [3]. Moreover, recently CaTiO_3 has shown a great interest in catalysis for oxidation of light hydrocarbons [4], in the field of luminescence [5] and in biocompatible applications [6].

Calcium titanate CaTiO_3 shares a combination of electrical, mechanical, thermal and optical characteristics. Meanwhile, CaTiO_3 undergoes a sequence of phase transitions: from a cubic ($\text{Pm}\bar{3}\text{m}$) to a tetragonal phase (I4/mcm) at $T \approx 1580 \text{ K}$, then to an orthorhombic phase (Pbnm) at $T \approx 1380 \text{ K}$ [7, 8]. For $T \geq 1580 \text{ K}$, CaTiO_3 has the ideal perovskite structure ($\text{Pm}\bar{3}\text{m}$). All of the structures are related to the ideal perovskite structure via small displacements of ions Ca^{2+} , Ti^{4+} and O^{2-} from their crystallographic positions.

At room temperature, CaTiO_3 crystallizes in a primitive orthorhombic lattice with 4 formula units per cell. The cell parameters are $a_0 \approx c_0 \approx \sqrt{2} a_c$ and $b_0 \approx 2a_c$, where a_c is the lattice parameter of the cubic perovskite phase. This structure is stable over a wide pressure and temperature region.

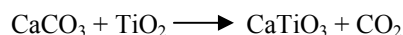
The purpose of this work is, first the preparation of new ceramics related to CaTiO_3 , chemically modified by MgF_2 and LiF . Second the investigation of the structural, microstructural, calorimetric and dielectric properties of the novel oxyfluorides.

2. Experimental procedure

2.1 Starting materials and pellet preparation

All used component were Merck products of 99.9 % purity or of suprapur quality. CaCO_3 and TiO_2 were previously dried at 150°C for 72 hours in order to eliminate water. The fluorides MgF_2 and LiF were dried by heating at 150°C under vacuum for 4h, in order to prevent hydrolysis during the sintering process.

The major constituent CaTiO_3 was previously prepared in air by the conventional solid-state reaction using CaCO_3 and TiO_2 (rutile). A stoichiometric mixture of these starting products was finely ground in an agate mortar then heat treated at 850°C for 8 hours.



Various molar mixtures $(1-x) \text{CaTiO}_3 + x \text{MgF}_2 + x \text{LiF}$ were prepared then dry-ground for approximately 30 min in an agate mortar. The powders thus obtained were pressed to discs of 13 mm diameter and about 1-2 mm thickness under an uniaxial pressure of 100 MPa. These pellets were sintered in air at 900°C for 2 hours on zircona plates with a heating rate of 200°C.h^{-1} .

2.2 X-ray diffraction

X-ray diffraction (XRD) analyses were carried out at room temperature on the sintered pellets crushed into fine powders. The data were collected in the angle range $5^\circ \leq 2\theta \leq 80^\circ$ using a philips PW 1710 diffractometer with the monochromatic radiation $\text{Cu}(\text{K}_{\alpha 1})$ ($\lambda = 1.54060 \text{ \AA}$). The unit cell parameters were determined and refined using a least squares refinement program.

3.2 SEM observations

The microstructures were characterized by scanning electron microscopy observations performed on fractured ceramics with an philips ESEM FEG XL30 apparatus using a voltage of 10 kV and various magnifications.

3.3 DSC analyses

Differential scanning calorimetry (DSC) analyses were carried out on crushed ceramics into fine powders over the temperature range 25 - 600 °C in the presence of nitrogen with a PERKIN-ELMER apparatus. The heating rate was 10 °C/min.

3.4 Dielectric measurements

Capacitors were prepared from pre-sintered pellets by depositing thin silver layers as electrodes onto the opposite circular faces. The dielectric study was performed at 100 Hz and 1 kHz from 500 °C to room temperature with a cooling rate of 5 °C/min. The measurements were carried out under nitrogen gas in a pyrex cell using a LCR data automatic bridge.

3. Results and discussion

3.1 X-ray diffraction study

The X-ray diffractometry study of the chemical system CaTiO_3 - MgF_2 - LiF at room temperature allowed us to identify a new solid solution $\text{Ca}_{1-x}\text{Mg}_x(\text{Ti}_{1-x}\text{Li}_x)\text{O}_{3-3x}\text{F}_{3x}$ with a perovskite structure. This occurs in the $0 \leq x \leq 0.25$ initial composition range. The figure 1 shows the X-Ray diffraction patterns of $\text{Ca}_{0.85}\text{Mg}_{0.15}(\text{Ti}_{0.85}\text{Li}_{0.15})\text{O}_{2.55}\text{F}_{0.45}$ phase.

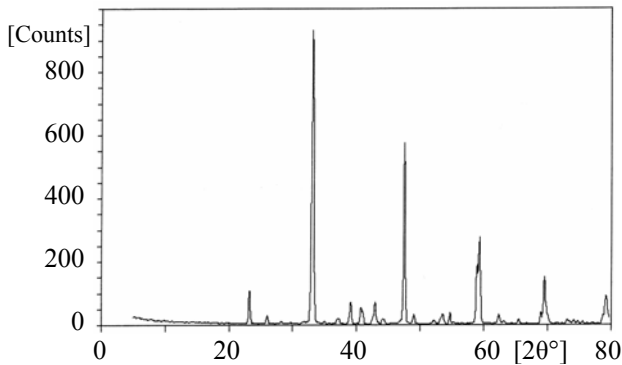


Figure 1: XRD pattern of $\text{Ca}_{0.85}\text{Mg}_{0.15}(\text{Ti}_{0.85}\text{Li}_{0.15})\text{O}_{2.55}\text{F}_{0.45}$

The peaks of X-ray patterns were indexed by comparison with the CaTiO_3 orthorhombic phase at room temperature. Table 1 gives respectively the unit cell parameters and the volume variation with composition.

$\text{Ca}_{1-x}\text{Mg}_x(\text{Ti}_{1-x}\text{Li}_x)\text{O}_{3-3x}\text{F}_{3x}$				
x	a [Å]	b [Å]	c [Å]	V [Å ³]
0.05	5.4449	7.6414	5.3846	224.0346
0.10	5.4341	7.6219	5.3448	221.3697
0.15	5.4431	7.6437	5.3810	223.8805
0.20	5.4681	7.6434	5.3836	225.0070
0.25	5.4674	7.6464	5.3640	224.2429

Table 1: XRD data of $\text{Ca}_{1-x}\text{Mg}_x(\text{Ti}_{1-x}\text{Li}_x)\text{O}_{3-3x}\text{F}_{3x}$ phases

The variation of the linear parameters and the unit cell volume with x is very low. This result could be attributed to the TiO_6 and LiF_6 octahedra which have almost the same size. Indeed, the cationic size increase from Ti^{4+} to Li^+ is compensated by the anionic size decrease from O^{2-} to F^- ($r_{\text{Ti}^{4+}} = 6.05$ nm; $r_{\text{Li}^+} = 7.4$ nm; $r_{\text{O}^{2-}} = 14$ nm; $r_{\text{F}^-} = 13.3$ nm in 6-coordination) [9].

3.2 Shrinkage and SEM observations

The linear shrinkages values $\Delta\Phi/\Phi$ (%) are reported in Table 2. The CaTiO_3 ceramic is very brittle after sintering at 900 °C for 2h. In the opposite, the $\text{Ca}_{1-x}\text{Mg}_x(\text{Ti}_{1-x}\text{Li}_x)\text{O}_{3-3x}\text{F}_{3x}$ ceramics are very hard and difficult to crush. Like the shrinkage, the relative density for the fluorinated samples increases with x and the values are in the range 92% - 98%.

Composition	$\Delta\Phi/\Phi$ (%)
CaTiO_3	5
$\text{Ca}_{0.95}\text{Mg}_{0.05}(\text{Ti}_{0.95}\text{Li}_{0.05})\text{O}_{2.85}\text{F}_{0.15}$	8.5
$\text{Ca}_{0.90}\text{Mg}_{0.10}(\text{Ti}_{0.90}\text{Li}_{0.10})\text{O}_{2.70}\text{F}_{0.30}$	14.6
$\text{Ca}_{0.85}\text{Mg}_{0.15}(\text{Ti}_{0.85}\text{Li}_{0.15})\text{O}_{2.55}\text{F}_{0.45}$	18.5
$\text{Ca}_{0.80}\text{Mg}_{0.20}(\text{Ti}_{0.80}\text{Li}_{0.20})\text{O}_{2.40}\text{F}_{0.60}$	20.3
$\text{Ca}_{0.75}\text{Mg}_{0.25}(\text{Ti}_{0.75}\text{Li}_{0.25})\text{O}_{2.25}\text{F}_{0.75}$	23.2

Table 2: Shrinkages of $\text{Ca}_{1-x}\text{Mg}_x(\text{Ti}_{1-x}\text{Li}_x)\text{O}_{3-3x}\text{F}_{3x}$ ceramics sintered at 900 °C for 2 h

No intergranular phases are observed in the SEM micrographs for all values of x. This result agrees quite well with the XRD study and implies that the ($\text{MgF}_2 + \text{LiF}$) additive simultaneously assists the sintering process and enters the CaTiO_3 lattice to form the solid solution $\text{Ca}_{1-x}\text{Mg}_x(\text{Ti}_{1-x}\text{Li}_x)\text{O}_{3-3x}\text{F}_{3x}$.

Typical micrographs for $\text{Ca}_{0.85}\text{Mg}_{0.15}(\text{Ti}_{0.85}\text{Li}_{0.15})\text{O}_{2.55}\text{F}_{0.45}$ are illustrated in Figure 2. As it may be seen, the grain morphology is not regular and its size is between ~ 1 μm and ~ 5 μm , with an inter-granular porosity.

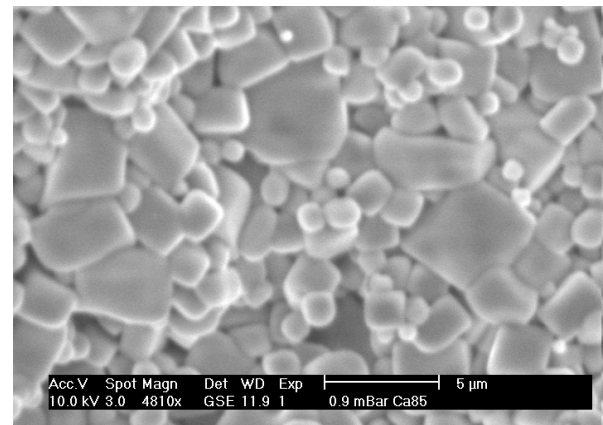


Figure 2: Microstructure of $\text{Ca}_{0.85}\text{Mg}_{0.15}(\text{Ti}_{0.85}\text{Li}_{0.15})\text{O}_{2.55}\text{F}_{0.45}$ ceramic sintered at 900 °C for 2h

3.3 DSC analyses

Two peaks are detected in $\text{Ca}_{1-x}\text{Mg}_x(\text{Ti}_{1-x}\text{Li}_x)\text{O}_{3-3x}\text{F}_{3x}$ phases for $x > 0.05$ in the temperature range investigated. On the other hand, only 1 calorimetric phenomenon is observed for $\text{Ca}_{0.95}\text{Mg}_{0.05}(\text{Ti}_{0.95}\text{Li}_{0.05})\text{O}_{2.85}\text{F}_{0.15}$ sample; the second one appears probably beyond 500 °C.

Small changes in enthalpy ΔH are associated to all the peaks and therefore these thermal anomalies are ascribed to second order structural transformations.

For example, Figure 3 gives the DSC curves of $\text{Ca}_{0.85}\text{Mg}_{0.15}(\text{Ti}_{0.85}\text{Li}_{0.15})\text{O}_{2.55}\text{F}_{0.45}$ where 2 phase transitions are clearly observed around 228 °C and 275 °C.

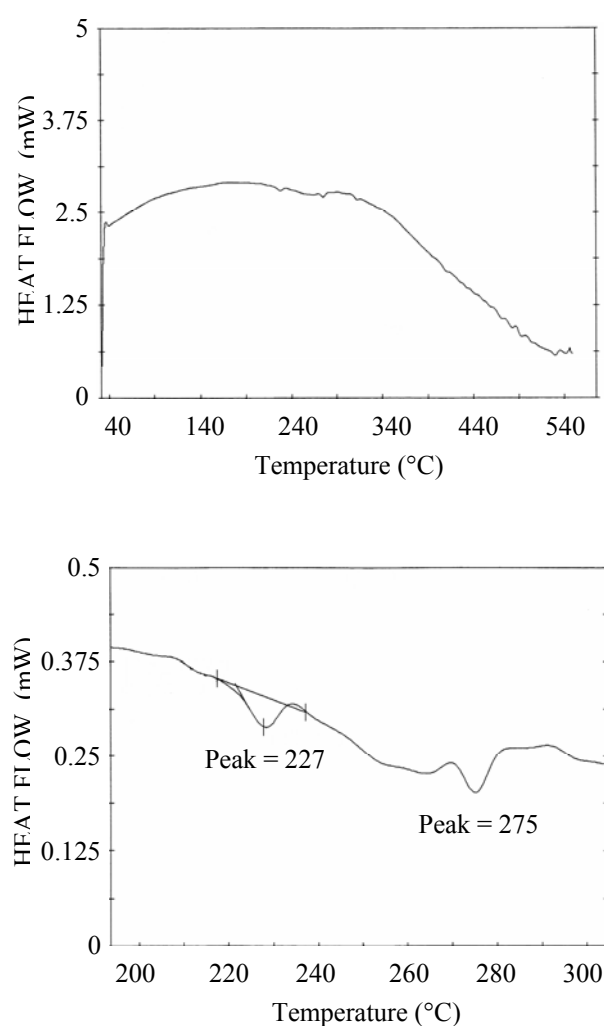


Figure 3: DSC curves of $\text{Ca}_{0.85}\text{Mg}_{0.15}(\text{Ti}_{0.85}\text{Li}_{0.15})\text{O}_{2.55}\text{F}_{0.45}$ sample sintered at 900 °C for 2h.

3.4 Dielectric measurements

The curves $\epsilon_r' - T$ and $\tan\delta - T$ of all the ceramics are similar to each other to matter the value of x or the

frequency (100 Hz or 1kHz). The permittivity ϵ_r' and the dielectric losses $\tan\delta$ are stable over a large range of temperature ($\sim 25 - 250^\circ\text{C}$) with a strong increase at higher temperatures. The phase transitions observed by DSC are confirmed by the dielectric measurements.

Figures 4 and 5 display the T - dependence of the dielectric permittivity and the dielectric losses at respectively 100 Hz and 1kHz for sample $\text{Ca}_{0.85}\text{Mg}_{0.15}(\text{Ti}_{0.85}\text{Li}_{0.15})\text{O}_{2.55}\text{F}_{0.45}$. Two dielectric phenomena are pointed out. These appear as slight shoulders and are more perceptible at 1 kHz (Figure 5).

The values of T_1 and T_2 are respectively 350 °C and 420 °C. They are much lower than reported for pure CaTiO_3 [7,8]. The decrease in the phase transitions temperatures is related to the diminishing of covalency in the bonds when oxygen O is substituted by fluorine F. The strong increase of ϵ_r' and $\tan\delta$ at high temperatures is mainly due to the electrical conductivity of lithium ion Li^+ .

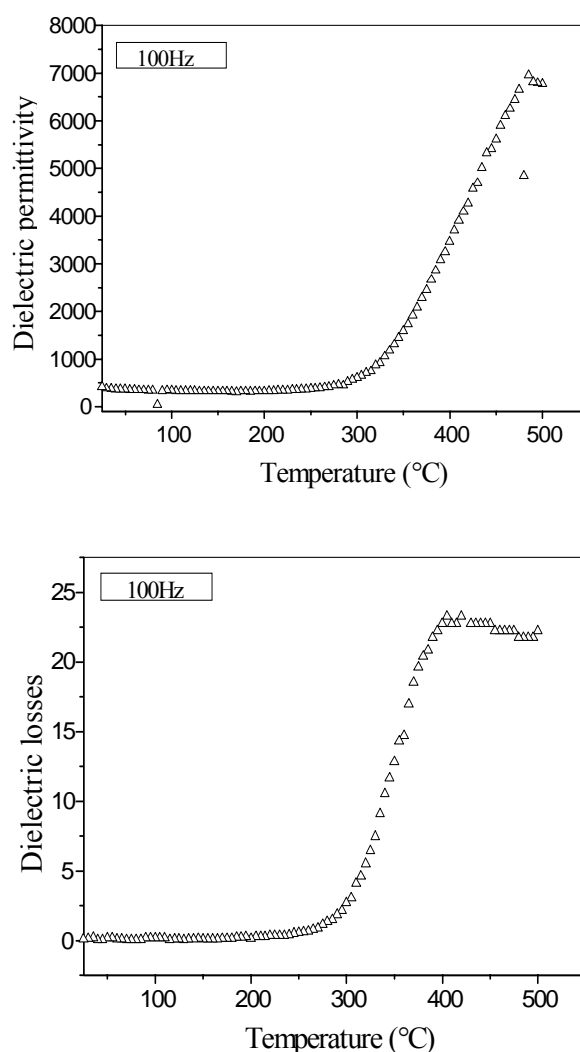


Figure 4 : Temperature dependence of ϵ_r' and $\tan\delta$ of $\text{Ca}_{0.85}\text{Mg}_{0.15}(\text{Ti}_{0.85}\text{Li}_{0.15})\text{O}_{2.55}\text{F}_{0.45}$ ceramic sintered at 900 °C for 2h (100Hz)

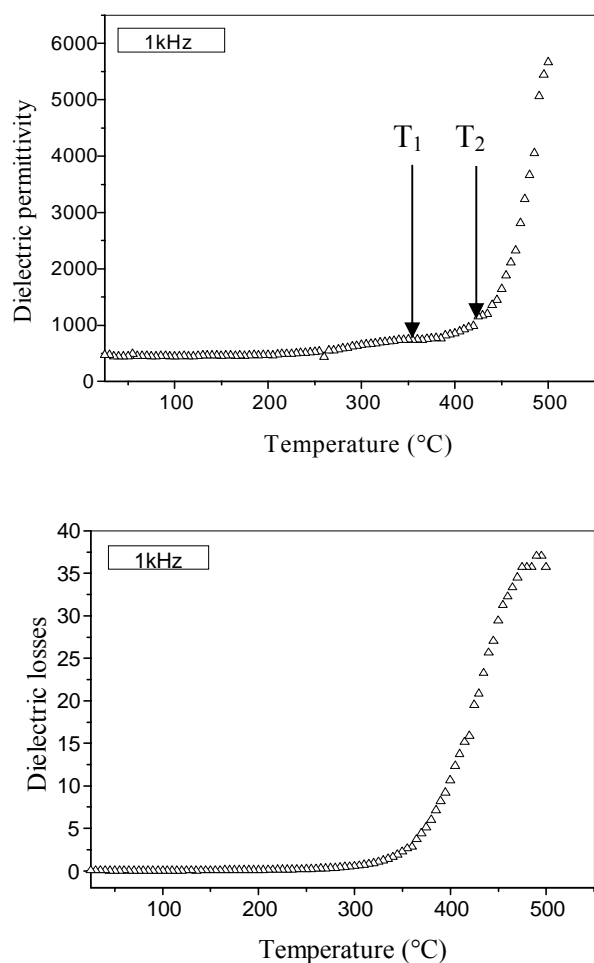


Figure 5: Temperature dependence of ϵ'_r and $\tan\delta$ of $\text{Ca}_{0.85}\text{Mg}_{0.15}(\text{Ti}_{0.95}\text{Li}_{0.05})\text{O}_{2.55}\text{F}_{0.45}$ ceramic sintered at 900°C for 2h (1 kHz).

The frequency dispersion in the permittivity and the dielectric losses is negligible between room temperature and approximately 250°C . Table 3 gives ϵ'_r and $\tan\delta$ values for 1 kHz at room temperature.

Composition	ϵ'_r	$\tan\delta$
$\text{Ca}_{0.95}\text{Mg}_{0.05}(\text{Ti}_{0.95}\text{Li}_{0.05})\text{O}_{2.85}\text{F}_{0.15}$	326	3.29
$\text{Ca}_{0.90}\text{Mg}_{0.10}(\text{Ti}_{0.90}\text{Li}_{0.10})\text{O}_{2.70}\text{F}_{0.30}$	67	0.37
$\text{Ca}_{0.85}\text{Mg}_{0.15}(\text{Ti}_{0.85}\text{Li}_{0.15})\text{O}_{2.55}\text{F}_{0.45}$	474	0.14

Table3: Values of ϵ'_r and $\tan\delta$ of $\text{Ca}_{1-x}\text{Mg}_x(\text{Ti}_{1-x}\text{Li}_x)\text{O}_{3-3x}\text{F}_{3x}$ for 1 kHz at 25°C

These results are in good agreement with our previous works on the oxyfluorides derived from CaTiO_3 [10-12].

4. Conclusion

A new solid solution $\text{Ca}_{1-x}\text{Mg}_x(\text{Ti}_{1-x}\text{Li}_x)\text{O}_{3-3x}\text{F}_{3x}$ ($0 \leq x \leq 0.25$) was obtained by the investigation of the chemical system CaTiO_3 - MgF_2 - LiF sintered at 900°C for 2h. The admixture of $(\text{MgF}_2 + \text{LiF})$ to CaTiO_3 lowers both the sintering temperature and the phase

transitions temperatures of pure calcium titanate. The fluorinated materials are orthorhombic at room temperature with a perovskite structure. The DSC analyses showed one or two thermal anomalies of second order. These phase transitions were confirmed by dielectric measurements.

Acknowledgements

The authors acknowledge Dr. A. Mezroua and Dr. N. Souami for their kind help in the sample characterizations.

References

- [1]. Preda M., Caldararu M., Dragan M.A., Concerning about synthesis and sintering of CaTiO_3 in presence of mineralisers, *Key Engineering Materials*, 2002, **206-213**, 147-150.
- [2]. Kutty T.R.N. and Vivekanandan R., Preparation of CaTiO_3 fine powders by the hydrothermal method, *Materials Letters*, 1987, **5 N°3**, 79-83.
- [3]. Levins D.M., Reeve K.D., Buykx W.J., Ryan R.K., Seatonberry B.W., Woolfrey J.L. and Hart P., *American Nuclear Society Int Meeting on Waste Management*, September 1986, Niagara Falls, NY.
- [4]. Andersen A.G., Hayakawa T., Tsunoda T., Orita H., Shimizu M. and Takehira K., Preparation and characterization of CaTiO_3 -based perovskitic oxides as catalysts for partial oxidation of light hydrocarbons, *Catalysis Lett.*, 1993, **18**, 37-48.
- [5]. Kang S.Y., Byun J.W., Kim J.Y., Suh K.S. and Kang S.G., Cathodoluminescence Enhancement of $\text{CaTiO}_3 : \text{Pr}^{3+}$ by Ga Addition, *Bull. Korean Chem. Soc.*, 2003, **24 N° 5**, 566-568.
- [6]. Manso M., Langlet M., Martinez-Duart J.M., Testing sol-gel CaTiO_3 coatings for biocompatible applications, *Materials Science and Engineering*, 2003, **C23**, 447-450.
- [7]. Becerro A.I., Redfern S.A.T., Carpenter M.A., Knight K.S. and Seifert F., Displacive Phase Transitions in and Strain Analysis of Fe-Doped CaTiO_3 Perovskites at High Temperatures by Neutron Diffraction, *Journal of Solid State Chemistry*, 2002, **167**, 459-471.
- [8]. Kennedy B.J., Howard C.J. and Chakoumakos B.C., Phase transitions in perovskite at elevated temperatures - a powder neutron diffraction study, *J. Phys. Condens. Matter*, 1999, **11**, 1479-1488.
- [9]. Shannon R.D., *Acta. Cryst.*, 1976, **A32**, 751.
- [10]. Cherfouh H., Mezroua A., Melouani B. and Benziada -Taïbi L., DSC and Dielectric Investigations in New Oxifluoride Ceramics $\text{Ca}(\text{Ti}_{1-x}\text{Li}_x)\text{O}_{3-3x}\text{F}_{3x}$, *Key Engineering Materials*, 2002, **206-213**, 1305-1308.
- [11]. Taïbi-Benziada L., Structural, thermal and dielectric studies of the solid solution $\text{Ca}_{1-x}\text{Sr}_x(\text{Ti}_{1-x}\text{Li}_x)\text{O}_{3-3x}\text{F}_{3x}$, *Solid State Phenomena*, 2003, **90-91**, 433-438.
- [12]. Mezroua A., Taïbi-Benziada L., Effects of processing parameters on the dielectric properties of $\text{Ca}(\text{Ti}_{0.95}\text{Li}_{0.05})\text{O}_{2.85}\text{F}_{0.15}$ ceramics, *Key Engineering Materials*, 2004, **264-268**, 1281-1284.